Machine Learning Aided Fan Broadband Interaction Noise Prediction for Leaned and Swept Fans

Nuo Li*
Boston University, Boston, MA, 02215, U.S.A.

Julian Winkler[†], Craig Aaron Reimann[‡], Dmytro Voytovych[§], Michael Joly[¶], Kin Gwn Lore[∥], Jeffrey M. Mendoza** *Raytheon Technologies Research Center, East Hartford, CT, 06108, U.S.A.*

Sheryl M. Grace^{††} *Boston University, Boston, MA, 02215, U.S.A.*

Fast prediction of the interaction broadband noise produced in a turbofan fan stage can benefit engine preliminary design. Over the years, multiple low-order methods for determining the unsteady response of the fan exit guide vane (FEGV) and related acoustics have been developed. These methods provide reasonable predictions of the interaction broadband noise when the fan wake flow upstream of the FEGV is known. The wake flow has been obtained previously from experiment, high fidelity computations and Reynolds Averaged Navier Stokes (RANS) simulations. In this paper, a machine learning method for obtaining the desired wake flow parameters is presented. The training database consists of 8 fan geometries that include varying lean and sweep with a total of 545 fan speed and mass flow cases. The database is generated using RANS. The efficacy of machine learning as a surrogate model for the wake is explored. The effect of inaccuracies in the learned wakes on the final acoustic prediction are noted. Noise outcomes due to varying fan lean and sweep are explored.

I. Introduction

The demand for more efficient and quieter aircraft continues to drive engine design. Broadband fan-stage interaction noise is a dominant source of noise in modern turbofan engines. The interaction noise is produced when the fan wake impinges on the FEGV. Methods for predicting this noise source during the design phase are of interest. Much research has focused on modeling the interaction noise [1, 2]. All of the methods assume that the flow upstream of the fan exit guide vane (FEGV) is known. The wake flow has been obtained previously from experiment, high fidelity computations and Reynolds Averaged Navier Stokes simulations. While the acoustics produced by the interaction may be computed quickly, obtaining the required wake flow parameters to be used as input into the acoustic prediction, renders the total method less useful for design. Therefore, this work focuses on developing a method for determining the wake flow parameters quickly. To this end, machine learning is being used as a surrogate model. The goal is to provide information about a fan's geometry and performance and allow the surrogate model to provide the necessary flow parameters upstream of the FEGV.

The first results for machine learned fan wake flow were reported in [3, 4]. Single and multiple output methods were considered originally and the multiple output method was selected. The fan used in the Source Diagnostic Test provided the initial geometries and a database with 268 cases was generated. Both deep neural and convolution neural networks were used to learn the circumferentially averaged axial and tangential mean flows, the turbulence intensity and the turbulence length scale with good outcomes. This paper begins to address the question of whether machine learning will work when the fan geometries differ more widely. As such, a series of leaned and swept fan blades have been created. A new database of 545 cases has been developed and machine learning has been tested on this new set of fans

^{*}Graduate Student, Mechanical Engineering Department, AIAA Student Member

[†]Sr. Principal Engineer, Acoustics, Aerothermal & Intelligent Systems Department, AIAA Associate Fellow.

[‡]Sr. Manager, Acoustics, Aerothermal & Intelligent Systems Department, AIAA Senior Member.

[§]Principal Engineer, Aerodynamics, Aerothermal & Intelligent Systems Department.

[¶]Sr. Principal Engineer, Aerodynamics, Aerothermal & Intelligent Systems Department.

Principal Engineer, Advanced Learning & Analytics, Aerothermal & Intelligent Systems Department.

^{**}Sr. Technical Fellow, Acoustics, Aerothermal & Intelligent Systems Department, AIAA Associate Fellow.

^{††}Associate Professor, Mechanical Engineering Department, AIAA Associate Fellow.

In this paper, some background on the machine learning method used in this work is discussed in Section II. A brief overview of the low-order acoustic prediction method applied in this work is also provided. More details concerning the machine learning method together with the development of the training data are given in Section III. Results are presented for the efficacy of machine learning as a surrogate model for the wake in Section IV. The noise associated with leaned and swept fans has also been explored and presented. The machine learning is shown to work well when predicting a fan whose geometry is "inside" the geometries in the database and works less well extrapolating to a design "outside" of the database.

II. Background

A. Machine learning applied to wakes

Machine learning (ML) has been applied to wake flows previously. Two dimensional flow downstream of a cylinder [5] has been considered. More closely related to the turbofan application is the learning of wakes downstream of wind turbines [6–8]. These utilized a deep neural network (DNN) to learn the total averaged flow at positions from the ground up to one rotor diameter above the turbine at locations downstream of the turbine. A recent work by Li [9] introduced the use of a Graphic Neural Network (GNN) which applies to a non-Euclidean space in order to learn the wake on a nonuniform grid downstream of the turbine.

The wake flow downstream of a fan has some similarity to the wind turbine problem except one can assume axisymmetry that does not exist for the wind turbine application. Also, in the current research, it is of interest to learn the circumferentially averaged values across a passage and not just the overall averaged value at a given radial location.

The previous fan wake ML research was limited to only the SDT R4 fan and its "hot" geometry variants [3, 4, 10]. The fans were very similar and as such their wakes at a given operating point were very similar. 7 fan speeds and about 10 mass flow rates for each geometry provided an ML training database of 268 cases; but it can be argued that there were really only 67 truly unique cases. An ML architecture that allowed for very accurate learning of the wake parameters of interest: streamwise velocity, turbulence kinetic energy and length scale was developed. It was shown that the wake flow at any certain mass flow rate along a speed line can be well predicted even when the entire speed line was removed from training database. It also showed that an entire fan geometry could be left out and then its wake flow predicted well. The previous research determined initial best practices for applying the machine learning to fan wakes. This includes

- learning the axial and tangential mean flow in two steps: DNN for the circumferentially averaged values at each radial locations; convolution neural network (CNN) for the full passage deficit.
- learning the turbulence length scale directly instead of learning TKE and ω separately then forming length scale
- utilizing batch normalization when training for better performance, except when training turbulence length scale
 In the prior research, it was also noted that including some input parameters such as the trailing edge boundary layer
 thickness did not improve the ML accuracy using the database containing only the SDT fan variants. However, as the
 size of training database increases requiring the ML model to resolve more complex features, such input parameters may
 be still considered.

B. Low-order FEGV response

The acoustic prediction is based on the semi-analytical model developed by Grace [2]. The turbulence interacting with the FEGV is modeled using a Liepmann spectrum which is why the fan wake turbulence intensity and length scale are necessary inputs. It uses strip theory in that a series of 2D cascade solutions are pieced together. The model allows for skewed gusts and computes the unsteady cascade response using the Ventres method [11] with added 3-D gust effect using the Graham similarity method [12]. The Green's function for an annulus is then applied to obtain the acoustic power in the exhaust duct. The method utilizes time averaged inflow parameters at 24-45 radial locations depending on the case. It is noted that some other low-order methods utilize the passage variation of the turbulence intensity. In the classification of broadband noise prediction models by Guerin et. al. [1] it is considered a Group A model.

III. Method

Four fan wake parameters just upstream of the FEGV leading edge location must be known in order to predict the FEGV broadband interaction noise: the axial and tangential mean velocity, the turbulence intensity and turbulence length scale. The ML database that includes this information for multiple fans, fan speeds and fan mass flow rates is obtained from RANS simulations. The two velocity components are extracted directly from the RANS simulation. The turbulence intensity is related to the turbulence kinetic energy. The turbulence length scale, Λ is estimated using Pope's [13] formula as a function of turbulence kinetic energy, k, and turbulence dissipation rate, ω :

$$\Lambda = 0.43 \frac{\sqrt{k}}{0.09\omega} \tag{1}$$

These flow parameters are specified on 30 axial slices evenly distributed between the trailing edge of the fan and the leanding edge of the FEGV. Each slice in the database is related to a given fan case through the ML inputs.

The inputs to the ML model are showed in Table 1. They relate to the fan geometry, operating condition, the fan flow profile, and the relative position of the slice in relation to the fan. The geometry and flow profile related inputs are specified at the 30 radial locations, except for M_{in} , which is uniform. The values of three flow parameters $(M_{in}, M_{out}, \alpha_{out})$ are computed by a meanline code AxStream. The relative axial location of fan trailing edge, \hat{x}_{TE} , is defined as $x - x_{TE}$, the axial distance between the fan trialing edge and the axial slice of interest in the interstage. The relative circumferential location of fan trailing edge, $\hat{\theta}_{TE}$, defined as $\frac{\theta_{TE} - \theta_{min}}{\theta_{max} - \theta_{min}}$ is the percentage of circumferential location of fan trailing edge relative to the passage of the interstage block in the RANS simulation, where θ_{max} and θ_{min} are the maximum and minimum circumferential position of the interstage block. The training inputs are concatenated into a 1×333 tensor. As such, the input data set can be represented by $X \in \mathbb{R}^{1\times N_c \times N_i \times 333}$. Where N_c is the total number of CFD cases and N_i is the number of slices in the axial direction.

Table 1 List of fan inputs for ML.

Input name	Size
Rotor speed	1 × 1
Mass flow rate	1×1
Relative axial location of rotor trailing edge, \hat{x}_{TE}	1×30
Relative circumferential location of rotor trailing edge, $\hat{\theta}_{TE}$	1×30
Rotor chord, c	1×30
Stagger angle, χ	1×30
Rotor camber angle, Φ	1×30
Rotor outlet flow angle, α_{out}	1×30
Rotor solidity, σ	1×30
Rotor inlet Mach number, M_{in}	1×1
Rotor outlet Mach number, M_{out}	1×30
Maximum profile thickness/chord ratio, Trelative	1×30
Maximum thickness of rotor profile, T_{max}	1×30
Outlet metal angle, Φ_{out}	1×30

545 CFD simulation cases representing 8 fans operating at 7 speedlines from 50% to 100% of 12657 RPM

are included in the training data set, each with 30 axial slices in the interstage gap. The 8 fan geometries are the SDT "cutback hot" fan, a baseline fan as shown in Fig.1, three baseline variants with added -10°, 15°, 30° degrees lean, and three baseline variants with added -15°, 15°, 20° degrees sweep. The variants are shown in Fig.2. While the SDT fan has different geometry and flow profile inputs compared to the baseline, the lean and sweep variants are only varied in $\hat{\theta}_{TE}$ and \hat{x}_{TE} compared to the baseline.

The training data is derived from fan-alone RANS simulations performed using a multi-block structured code (UTCFD) with $219\times97\times145$ grid at the interstage block. The turbulence is modeled using the $k-\omega$ -model of Wilcox[14]. More information has been given in [3]. For our method, i.e. training 3-D data via 2-D CNN model, it is convenient to use data in a uniform grid. This allow us to specify an axial location for each slice and embed it in \hat{x}_{TE} . As such, the CFD results are interpolated into a $30\times50\times30$ grid in axial, circumferential, and radial locations. A coarse, uniform grid also has the benefits of reducing the ML training cost and ensuring that training loss is unbiased relative to the location.



Fig. 1 Comparison of SDT R4 fan and new fan design. Red: SDT. Black: New fan design

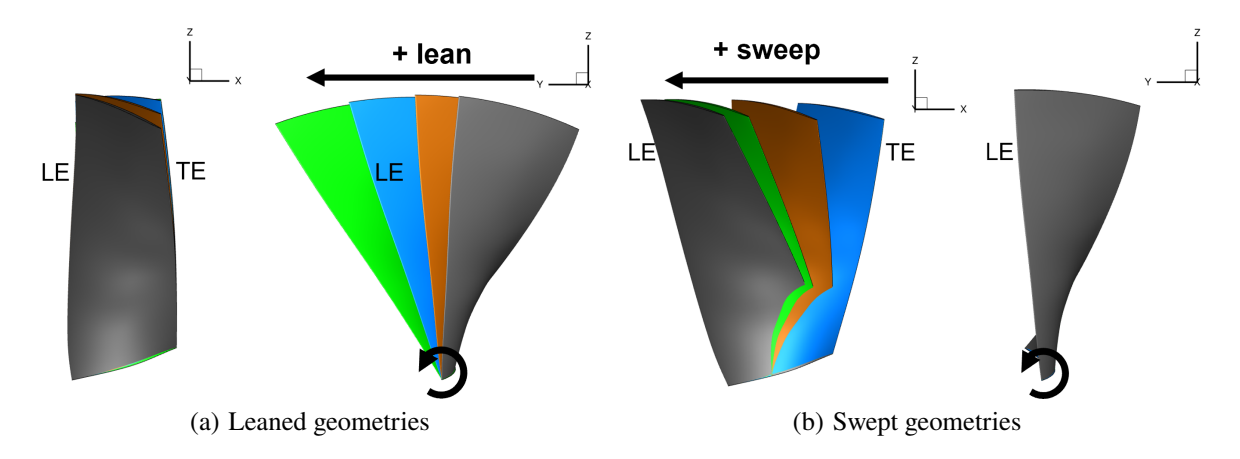


Fig. 2 New baseline fan geometries. Leaned: Grey: -10°, Brown 0° (baseline), Blue: +15°, Green:+30°. Swept: Blue: -15°, Brown 0° (baseline), Green: +15°, Grey: +20°.

A modified architecture based on the the previous work [4] is applied. The structure is based on a 2-D CNN model described in Fig. 3 and the detailed model parameters are explained in Tables A1, and A2. While the model in [4] has 7 deconvolutional layers, it was found that with new geometries in the database, adding an additional deconvolutional layer considerably decreases the test mean absolute error. Previous study found that adding batch normalization layers between deconvolutional layers improves the performance of training v_x , v_t and TKE when the database contains only the SDT variants. However, when switching to the new training database, it was found that the training and testing accuracy is adversely affected and therefore, the batch normalization layer is turned off. This may be caused by uneven training inputs, wherein the majority of the input parameters of the new baseline fan variants are the same, but substantially differ from the SDT fan present in the new database. The concatenated input tensor is transformed into a 1×84 tensor by two fully-connected layers, which can be conveniently reshaped into a 7×12 feature map, and can be then transformed into a 28×50 output layer via 8 deconvolutional layers. Each output image represents the prediction of an axial slice in a case. For each flow parameter, the total data set can then be denoted by $Y_{CNN} \in \mathbb{R}^{N_c \times N_i \times N_j \times N_k}$, where N_i and N_k are the number of points in circumferential and radial direction for each slice.

The DNN model explained in Table A3 is utilized to reinforce the training for axial and circumferential velocity. To train these parameters, the averaged background values and the deficits are separated. The circumferentially averaged values at every radial location are learned by the DNN model with four hidden layers using the same 1×333 inputs. The DNN output, which has the dimension of $1\times N_k$ in every axial slice for each veolocity component is then combined with the velocity deficits learned by CNN to obtain the final axial and circumferential velocity.

The learning rate is manually tuned by trial-and-error. When training velocity deficits and turbulence kinetic energy

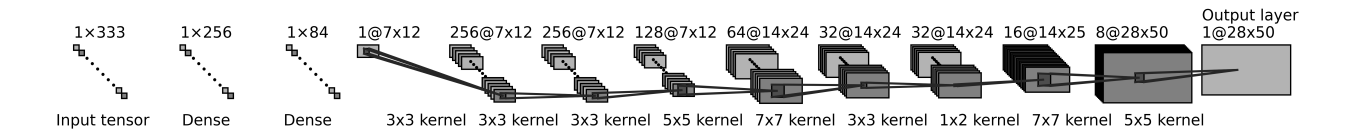


Fig. 3 CNN architecture

using CNN, a slight improvement is observed when a dynamic learning rate is employed. Therefore, a simple step-based decaying learning rate function is applied:

$$\eta_n = \eta_0 \cdot 0.94^{\frac{1+n}{r}} \tag{2}$$

where η_n denotes the learning rate at current iteration step, η_0 is the initial learning rate set to 0.005 for turbulence kinetic energy and 0.002 for velocity deficits. n is the current step number, and r is the decay step which is set to 300. This method requires multiple trials to find the optimum decay parameters. Fixed learning rates are used in the DNN model for the mean velocities and the CNN model for the turbulence length scale as the dynamic learning rate had little to no improvement.

IV. Results

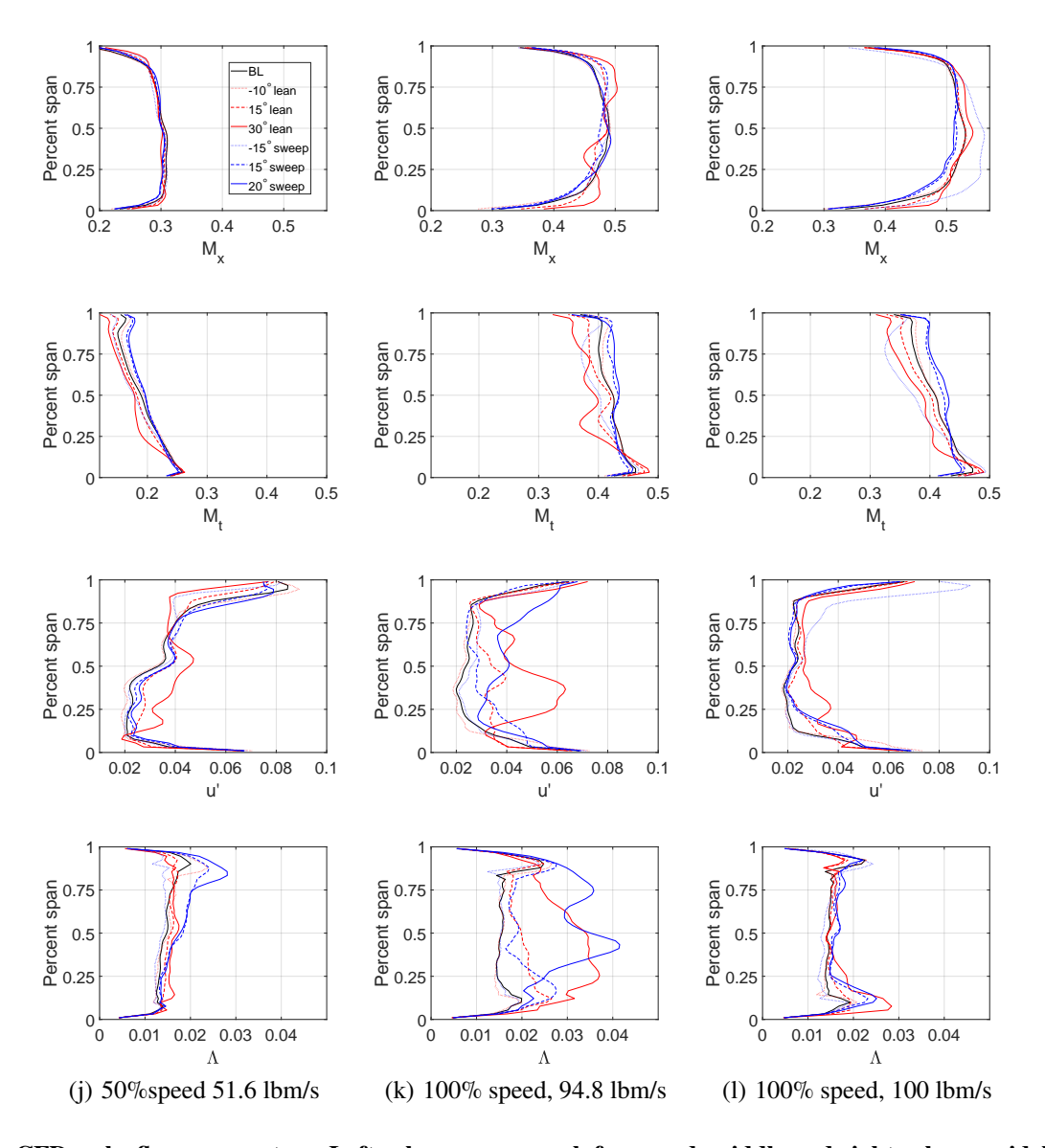
A. Wake Behavior and Acoustic Trends

Before addressing the ML aspect of the research, the RANS database is used to investigate the effect of fan lean and sweep on the fan wake and the broadband fan stage noise. Flow values are specified at 45 radial strips at the axial location coincides with the SDT HW2 location, where the experimental measurements were acquired. Fig. 4 shows the circumferentially averaged normalized wake parameters for the baseline fan and its leaned and swept variants taken directly from the RANS simulations. The axial and tangential Mach numbers (Mach number based on downstream temperature) are shown in the top two rows. The turbulence is assumed to be homogeneous so that the turbulence intensity, u' is found by $\sqrt{\frac{2}{3}TKE}$, and is normalized by the streamwise velocity. The turbulence length scale, Λ is normalized by the duct radius.

All of the geometries show somewhat similar Mach number at low speed. Forward lean appears to create more turbulent flow at the mid-span but less turbulence near the tip. The sweep design has a large effect on the turbulence length scale especially near the tip. This is possibly due to the change in axial distance between fan trailing edge and the axial slice of interest, which affects the turbulence development.

The interaction broadband noise produced by the different fan geometries with the same baseline FEGV geometry is shown in Fig. 5. Past studies [2, 10] have found that turbulence length scale tips the spectrum. As such, the forward sweep fans have higher sound power at low speed. This is shown in Fig. 5(a).

At high speeds, both adding forward lean and forward sweep result in much higher u' and Λ at low mass flow rate leading to higher sound power level as shown in Fig.5 (b). As mass flow rate increases, the u' and Λ become less sensitive to lean and sweep, but the wake flow coming out of the backward sweep fan is comparably more axial which also contributes to higher noise. The sound power spectra at a higher mass flow rate is plotted in Fig.5 (c).



 $\begin{tabular}{ll} Fig.~4 & CFD~wake~flow~parameters.~Left~column approach~fan~speed,~middle~and~right~columns~sideline~fan~speed. \end{tabular}$

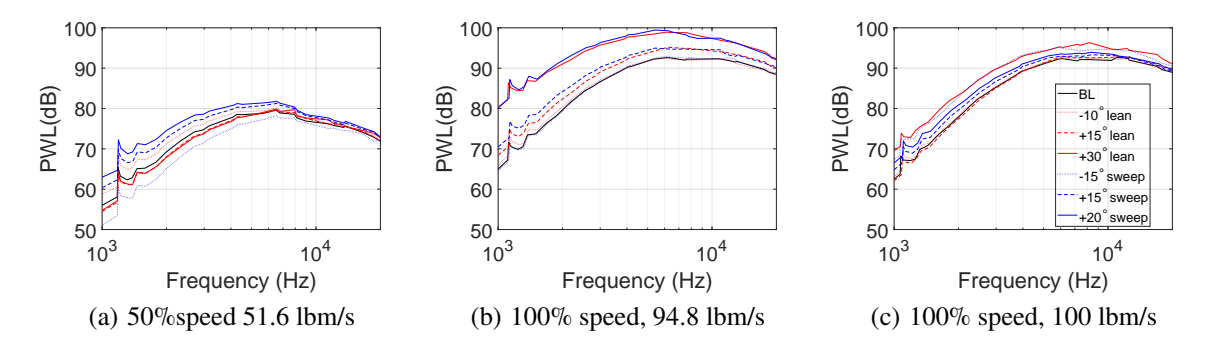


Fig. 5 PWL spectrum computed using inputs obtained from CFD.

To compare the overall sound power trends, the integral averaged sound power level is computed across the spectrum for all cases and shown in Figs. 6 & 7 for leaned and swept fans. The adiabatic efficiency is also provided. The optimal flow rate for acoustic does not perfectly mirror the highest adiabatic efficiency, and appears to be slightly shifted toward the lower mass flow rate. However, the efficiency and acoustic have fairly consistent trends when compared across the fan design. The lean variation has a small impact on the acoustic at low speeds. At higher speeds, forward lean produces more noise and larger variation with respect to mass flow rate. Sweep has the effect of shifting both acoustic and efficiency curves, where the forward sweep shifts the optimal point toward higher mass flow rates and backward sweep shifts the optimal point toward lower mass flow rate. Within a speed line, high efficiency roughly equates to lower noise. From speedline to speedline however, the maximum efficiency does not change much while the broadband noise changes drastically, increasing with speed.

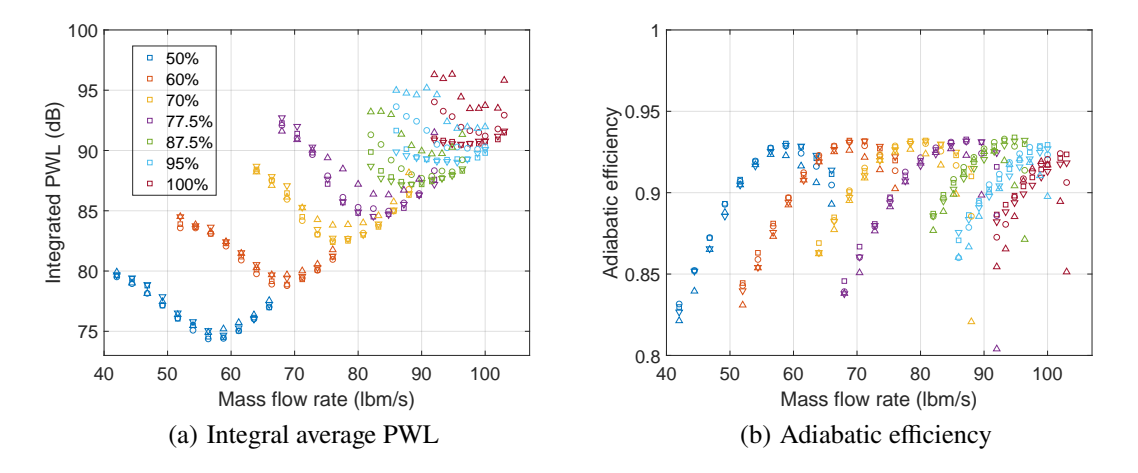


Fig. 6 Integral averaged PWL and adiabatic efficiency baseline and leaned fans. Downward triangles: -10° . Squares: 0° (BL). Circles: 15° . Upward triangles: 30°

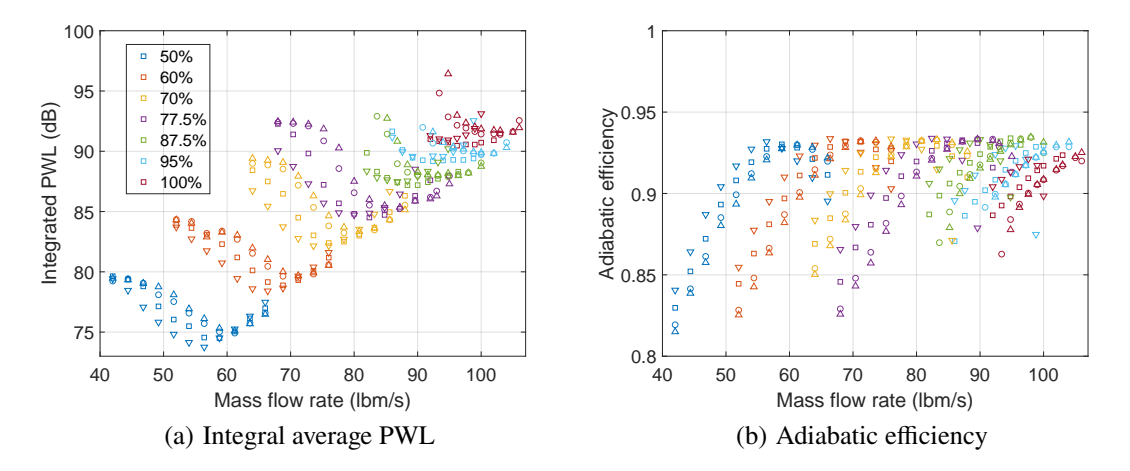


Fig. 7 Integral averaged PWL and adiabatic efficiency for baseline and swept fans. Downward triangles: -15° . Squares: 0° (BL). Circles: 15° . Upward triangles: 20°

B. ML Predicted Wake and Acoustic Trends for Leaned and Swept Fans

The ML model is first tested by reserving a random set of 20% of the cases for testing and using the other 80% for training and validation. The reserved cases cover all 8 fans at every speed line. Fig. 8 shows the predicted wake parameters from an example case that represents a typical outcome. Both the CFD and ML predicted values are interpolated onto a 28×50 axial slice (two radial locations are removed due to the solid wall condition). The plots show that ML can precisely capture the wake shape of the passage with relatively small error.

To further assess the model. A full fan geometry can be removed from the training set. Four tests were run leaving out an entire fan geometry: two fans with intermediate lean and sweep angles, 15° lean and 15° sweep; the fan with the largest lean angle, 30° lean; and the fan with the lowest sweep angle, -15°. These fans are reserved one at a time with all cases associated with that fan being removed from the training dataset. An example case is shown in Fig. 9 when the 15° sweep cases are reserved. The results show that ML is capable of predicting the wake of a fan with sweep variation if the sweep angle is within the range of fan geometries used for training the ML. When the 30° lean fan is reserved, the test results show that the model typically overpredicts the axial velocity and the turbulence kinetic energy as shown in Fig. 10. It also predicts the wake width incorrectly.

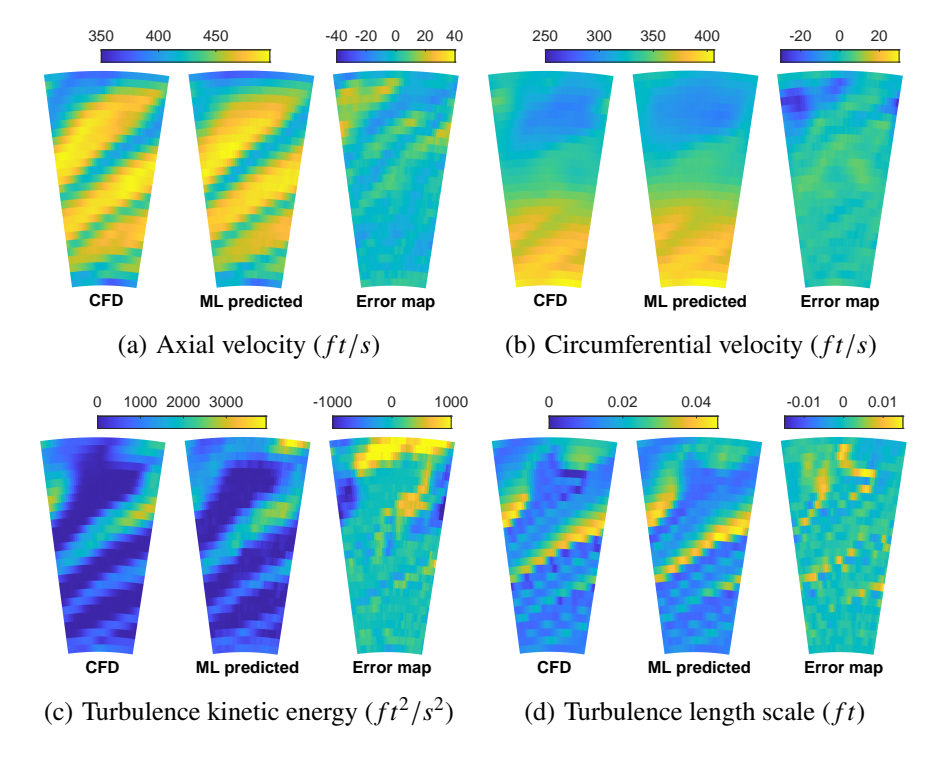


Fig. 8 ML test prediction using random evaluation method. Evaluation slice taken at HW2 location. SDT cutback hot operating at 77.5% speed, 72.8 lbm/s.

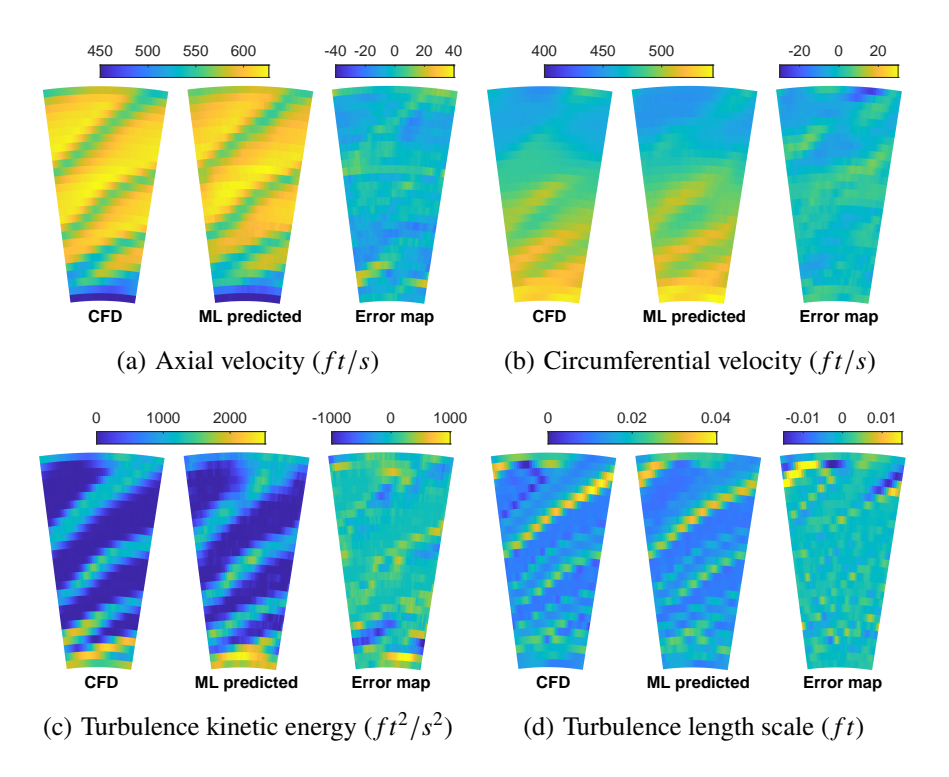


Fig. 9 ML test prediction when 15° sweep fan cases are removed. Evaluation slice taken at HW2 location. 15° sweep fan operating at 100% speed, 100 lbm/s.

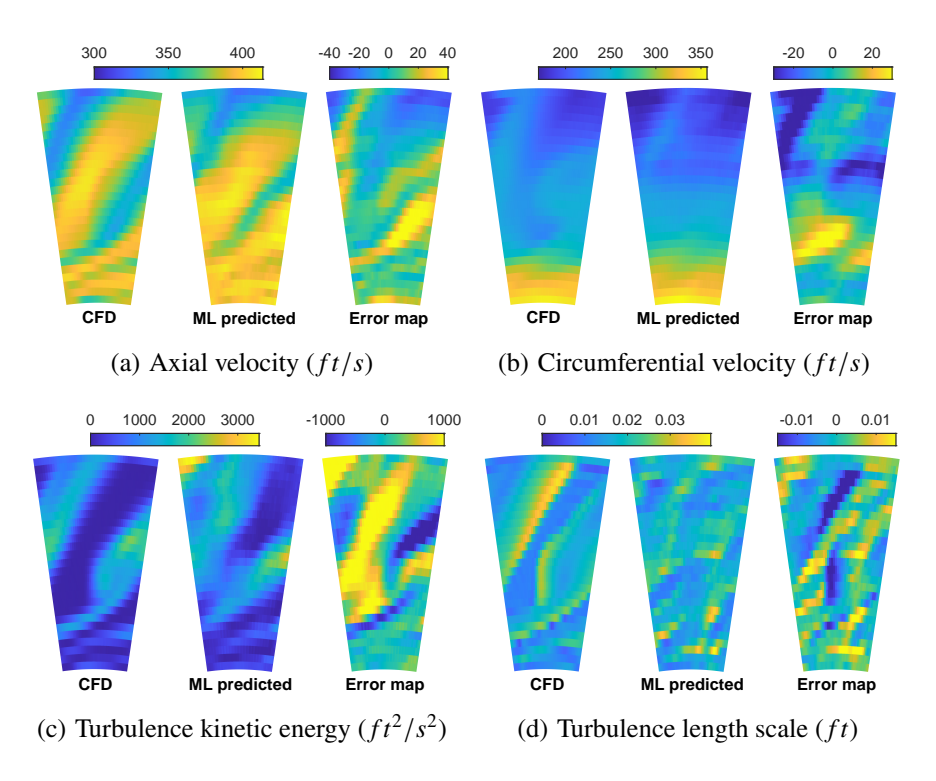


Fig. 10 ML test prediction when 30° lean fan cases are removed. Evaluation slice taken at HW2 location. 30° lean fan operating at 60% speed, 59.2 lbm/s.

The circumferentially averaged flow parameters that serve as the inputs for the acoustic prediction are shown in normalized form in Fig. 11 for the example cases described in Figs. 8, 9 and 10. Both the random evaluation and the 15° sweep test cases agree very well with the CFD results. The 30° lean test case exhibits comparatively greater discrepancies especially in u'.

Fig. 12 shows the computed acoustic spectra of these cases, the results also reflect the aforementioned ML outcomes, with the largest error occurring when the 30° lean fan is reserved. This is expected because reserving the 30° lean fan requires the ML model to extrapolate and the turbulence behavior is nonlinear with respect to the fan design.

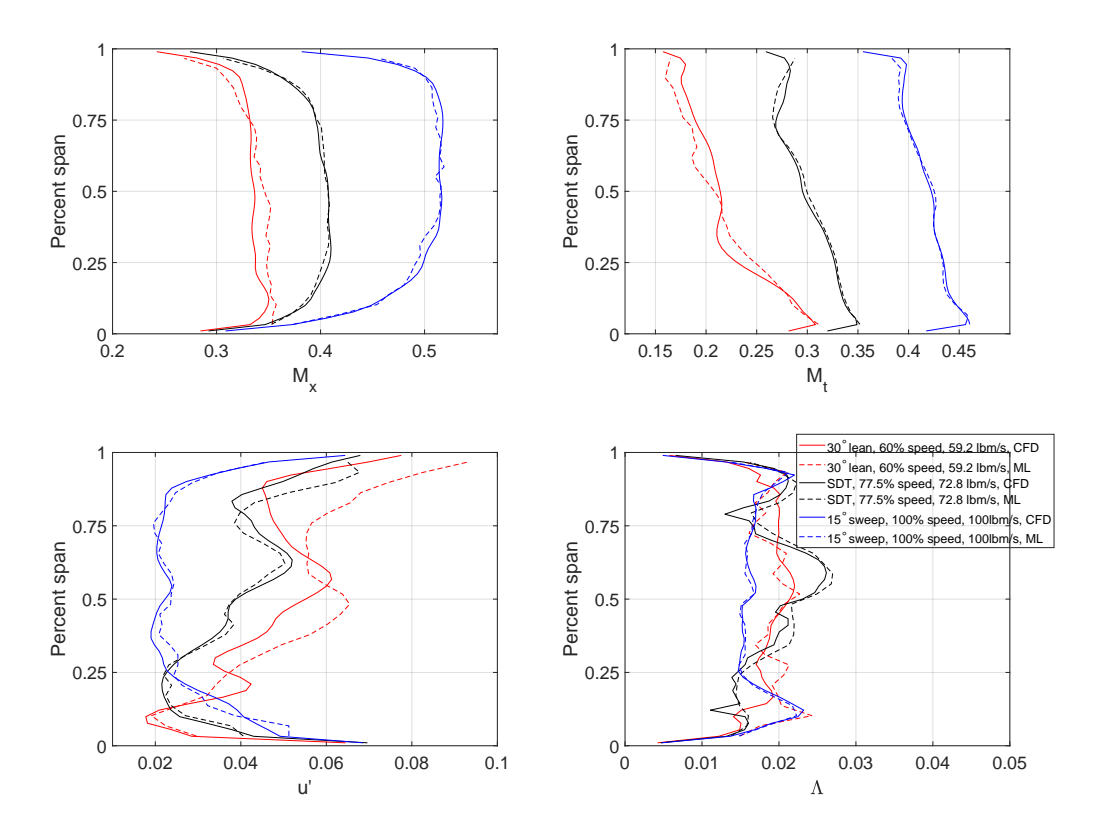


Fig. 11 CFD (solid) and ML (dashed) predicted circumferentially averaged acoustic input. Black: random evaluation, SDT fan at 77.5% speed, 72.8 lbm/s. Blue: 15° sweep fan reserved, 100% speed, 100 lbm/s. Red: 30° lean fan reserved, 60% speed, 59.2 lbm/s.

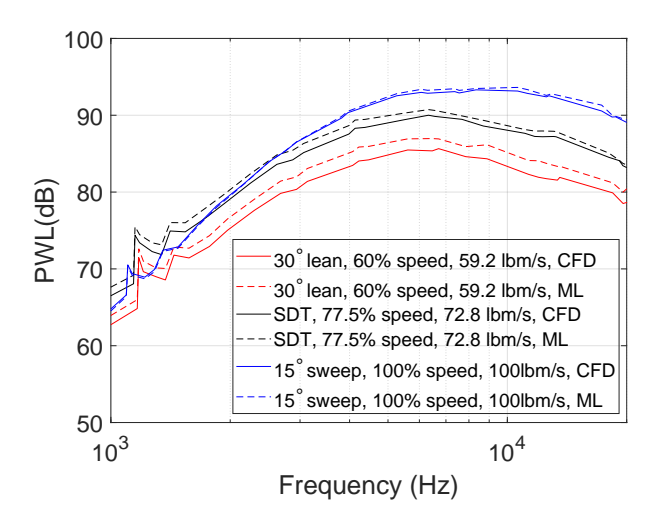


Fig. 12 PWL spectrum using CFD (solid) and ML (dashed) predicted inputs. Black: random evaluation, SDT fan at 77.5% speed, 72.8 lbm/s. Blue: 15°sweep fan reserved, 100% speed, 100 lbm/s. Red: 30°lean fan reserved, 60% speed, 59.2 lbm/s.

The integral averaged PWL is again calculated to measure the overall accuracy of ML predictions. Fig. 13 shows the values computed using CFD and ML predicted inputs when 20% of the cases are randomly reserved for testing. The ML predicted acoustic outcomes are in good agreement with the acoustic predictions computed using inputs directly from the CFD. Most cases exhibit less than 1 dB error. The acoustic results based on machine learned values for a fan not included in the training set are shown in Fig. 14. In this figure, the circles denote intermediate geometries (15° lean and 15° sweep) results using CFD input, and the crosses represent results using ML predicted inputs. The triangles are marginal geometries (30° lean and -15° sweep) results using CFD inputs, and the corresponding ML predicted results are represented by asterisks. These results exhibit small error when an intermediate fan is removed, i.e. 15° sweep and 15° lean, but relatively large error when the model has to extrapolate, i.e. -15° sweep and 30° lean. Specifically, all 30° leaned fan cases are overpredicted, and the -15° sweep fan cases show good agreement at low speed but are overpredicted at high. The overall mean errors are 0.2788 dB for 15°sweep fan, 1.1441 dB for -15°sweep fan, 0.3650 dB for 15°lean fan, and 1.2724 dB for 30°lean fan. Notably, even when the ML model has to extrapolate the flow parameters from outside of the fan designs included in the training set, the acoustic predictions based on these inputs still capture the trends very well.

The mean error averaged over each speed line for all of the test cases is shown in Fig. 15. The mean prediction error increases with fan speed when the -15° swept fan is reserved, whereas it decays when the 30° leaned fan is reserved. However, when evaluated randomly or with an intermediate fan design, the error does not appear to be strongly related to fan speed.

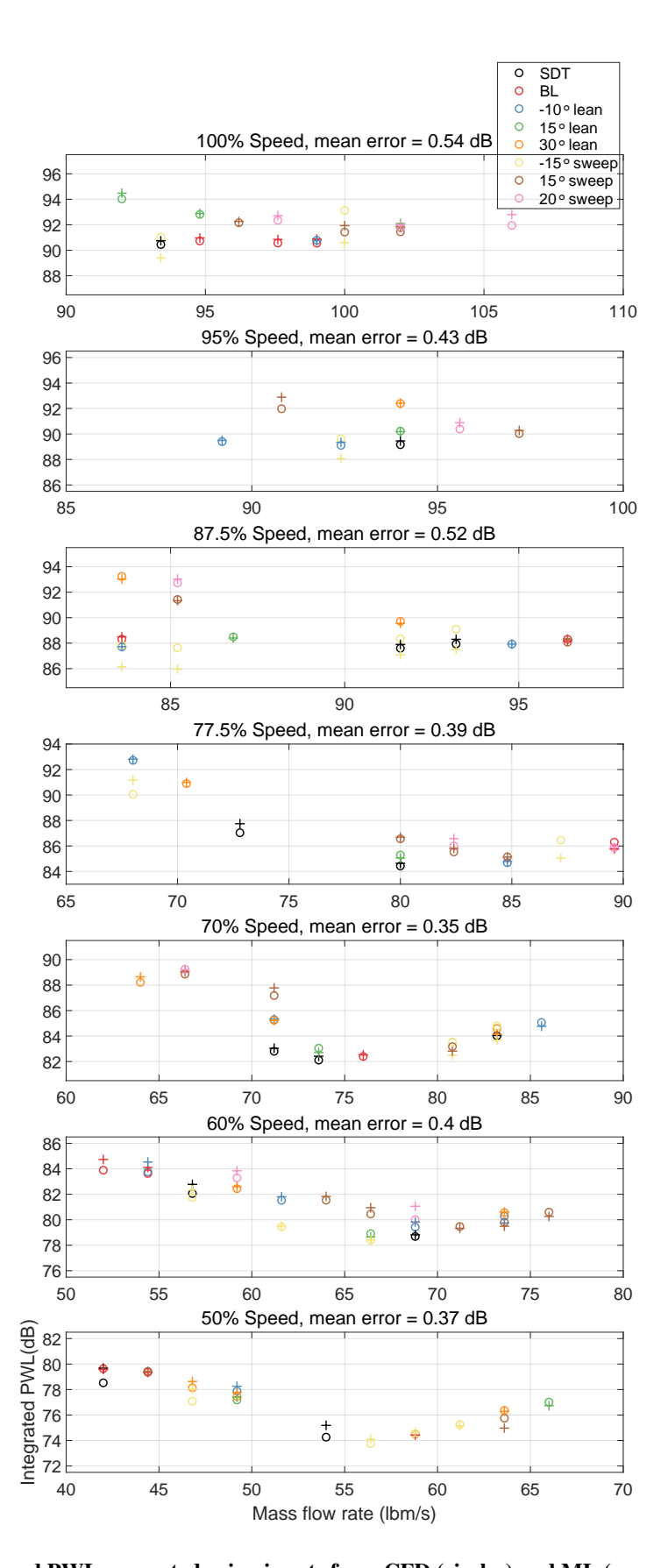


Fig. 13 Integral averaged PWL computed using inputs from CFD (circles) and ML (crosses) random evaluation set. Overall mean error is $0.4313 \ dB$.

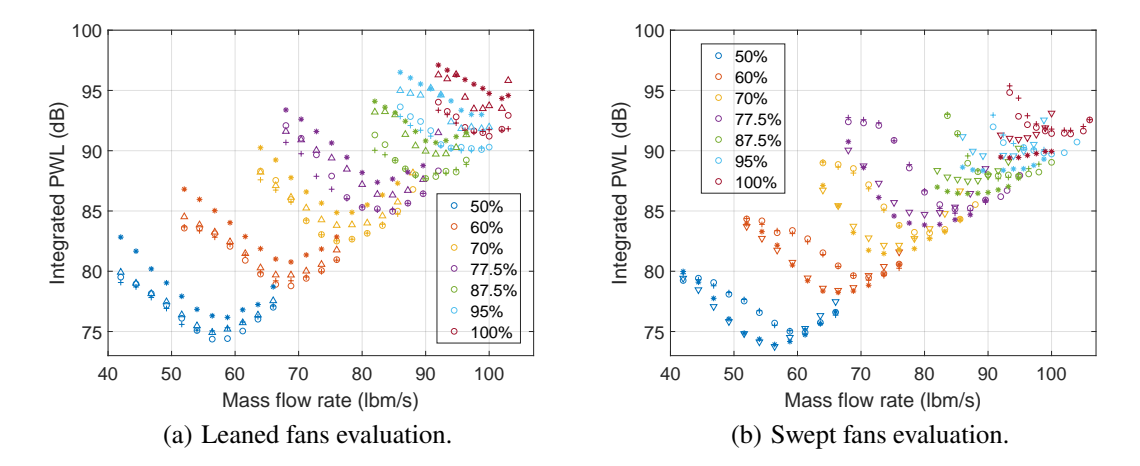


Fig. 14 Integral averaged and maximum sound power level when two leaned fans and two sweep fans are reserved for evaluation separately.

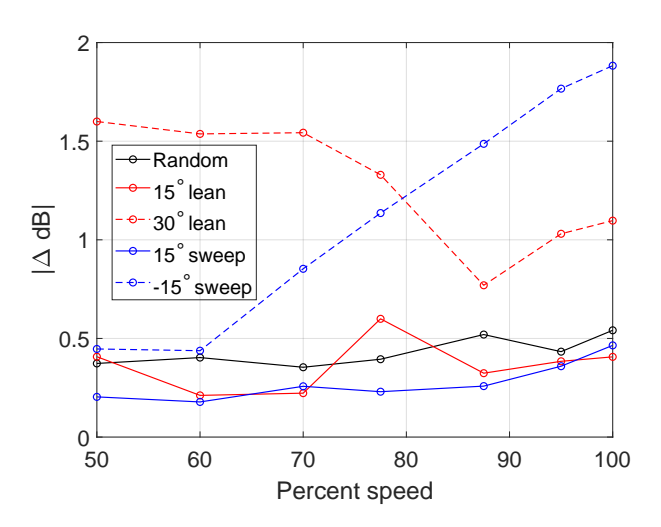


Fig. 15 Mean error in dB as function of percent speed for five evaluation batches. Dashed line represents an extrapolation case.

V. Conclusions

A hybrid fan-stage broadband interaction noise prediction method that couples machine learning (ML) of the fan wake with a semi-analytical acoustic model is improved and further analyzed using a larger database consisting of fans with varying lean and sweep. The ML outcomes showed that the model can predict the fan wake flow values when trained using random fan speed and mass flow rate combinations or when trained with full fan geometries excluded. The ML's prediction accuracy is lower for fans with geometry parameters that lie outside of the range of geometry parameters represented in the training data set. Still, the final acoustic trend predictions are reasonable across speed lines even for an extrapolated fan geometry.

Future efforts will expand the training database to include fan designs with different blade count and diameter. The selection of input parameters and their influence on the model's predictions will also be further investigated.

Acknowledgments

This research was funded by the U.S. Federal Aviation Administration Office of Environment and Energy through ASCENT, the FAA Center of Excellence for Alternative Jet Fuels and the Environment, project 75 through FAA Award Number 13-C-AJFE-BU under the supervision of Christopher Dorbian. Any opinions, findings, conclusions or recommendations expressed in this material are those of the authors and do not necessarily reflect the views of the FAA. Additional funding has come from RTRC and the BU Mechanical Engineering Department. The development of the low-order acoustic method was funded through the Ohio Aerospace Institute on a grant from the AeroAcoustics Research Consortium.

Appendix: ML model structure

Table A1 CNN layer parameters for velocity deficit, turbulence kinetic energy and length scale.

Structure	Numbers of feature maps	Size of feature map	Size of kernel	Stride
Fully connected layer-1	256	1×1	/	/
Fully connected layer-2	84	1×1	/	/
Transposed 2D convolution layer-1	256	7×12	3×3	1×1
Transposed 2D convolution layer-2	256	7×12	3×3	1×1
Transposed 2D convolution layer-3	128	7×12	3×3	1×1
Transposed 2D convolution layer-4	64	14×24	5×5	2×2
Transposed 2D convolution layer-5	32	14×24	7×7	1×1
Transposed 2D convolution layer-6	32	14×24	3×3	1×1
Transposed 2D convolution layer-7	16	14×25	1×2	1×1
Transposed 2D convolution layer-8	8	28×50	7×7	2×2
Output layer	1	28×50	5×5	1×1

Table A2 CNN model parameters for velocity deficit, turbulence kinetic energy and length scale.

Parameter	Value
Activation function at hidden layer	LeakyReLU
Optimizer	Adam
Learning rate	0.0005 and dynamic
Objective function	Mean squared error
Metrics	Mean absolute error
Batch size	256

Table A3 DNN model parameters for mean axial and circumferential velocity.

Parameter	Value
Input size	1×333
Number of neurons in hidden layer-1	512
Number of neurons in hidden layer-2	256
Number of neurons in hidden layer-3	128
Number of neurons in hidden layer-4	64
Number of neurons in output layer	28
Activation function at hidden layer	LeakyReLU
Optimizer	Adam
Learning rate	0.0002
Objective function	Mean squared error
Metrics	Mean absolute error
Batch size	256

References

- [1] Guérin, S., Kissner, C., Seeler, P., Blázquez, R., Carrasco Laraña, P., Laborderie, H., Lewis, D., Chaitanya, P., Polacsek, C., and Thisse, J., "ACAT1 Benchmark of RANS-Informed Analytical Methods for Fan Broadband Noise Prediction: Part II—Influence of the Acoustic Models," *Acoustics*, Vol. 2, 2020, pp. 617–649.
- [2] Grace, S., "Fan Broadband Interaction Noise Modeling Using a Low-Order Method," *Journal of Sound and Vibration*, Vol. 346, 2015, pp. 402–423.
- [3] Huang, Z., Shen, H., Kung, K., Luis Carvalho, A. T., Watchmann, B., Ramsarran, T., Winkler, J., Reimann, A., Joly, M., Lore, K. G., Mendoza, J., and Grace, S. M., "Investigation of Sound Generation and Transmission Effects Through the ACAT1 Fan Stage using Compressed Sensing-based Mode Analysis," AIAA Paper No. 2022-2883, 2022. doi:10.2514/6.2022-2883.
- [4] Li, N., Zhang, Y., Winkler, J., Reimann, A., Voytovych, D., Joly, M., Lore, K. G., Mendoza, J., and Grace, S. M., "Development of fully low-order predictions of fan broadband interaction noise via integration of machine learning," *AIAA Journal*, in review.
- [5] Fukami, K., Fukagata, K., and Taira, K., "Super-resolution reconstruction of turbulent flows with machine learning," *Journal of Fluid Mechanics*, Vol. 870, 2019, pp. 106–120. doi:10.1017/jfm.2019.238.
- [6] Renganathan, S. A., Maulik, R., Letizia, S., and Iungo, G., "Data-Driven Wind Turbine Wake Modeling via Probabilistic Machine Learning," *Neural Computing and Applications*, 2021.
- [7] Ti, Z., Deng, X., and Yang, H., "Wake modeling of wind turbines using machine learning," *Applied Energy*, Vol. 257, 2020, p. 114025. doi:10.1016/j.apenergy.2019.114025.
- [8] Anagnostopoulos, S., and Piggott, M., "Offshore wind farm wake modelling using deep feed forward neural networks for active yaw control and layout optimisation," *Journal of Physics: Conference Series*, Vol. 2151, 2022, p. 012011. doi:10.1088/1742-6596/2151/1/012011.
- [9] Li, S., Zhang, M., and Piggott, M., "End-to-end Wind Turbine Wake Modelling with Deep Graph Representation Learning," *Applied Energy*, Vol. 339, 2023. doi:10.1016/j.apenergy.2023.120928.
- [10] Li, N., Watchmann, B., Ramsarran, T., Winkler, J., Reimann, A., Voytovych, D., Mendoza, J., and Grace, S. M., "Fan-stage broadband interaction noise trends," *AIAA Paper No.* 2022-2884, 2022. doi:10.2514/6.2022-2884.
- [11] Ventres, C., Theobald, M. A., and Mark, W. D., "Turbofan Noise Generation Volume 1: Analysis," Tech. Rep. CR-167952, NASA, July 1982.
- [12] Graham, J. M. R., "Similarity rules for thin aerofoils in non-stationary subsonic flows," *Journal of Fluid Mechanics*, Vol. 43, 1970, pp. 753–766.

- [13] Pope, S. B., Turbulent Flows, Cambridge University Press, Cambridge, UK, 2000.
- [14] Wilcox, D. C., Turbulence modeling for CFD, DCW industries, Canada, 1998.